

# Magnetic and luminescent dual-functional SiO<sub>2</sub> beads created through controlled sol-gel process

Zhongsen Yang\*

State Key Laboratory of Crystal Materials, Shandong University, Jinan 250100, P. R. China

\*Corresponding author. Tel: (+86) 531 88361206; Fax: (+86) 531 88364864; E-mail: zsyang@sdu.edu.cn

Received: 14 Jan 2011, Revised: 20 Feb 2011 and Accepted: 08 May 2011

## ABSTRACT

A controlled sol-gel approach was developed to encapsulate luminescent CdTe and magnetic Fe<sub>3</sub>O<sub>4</sub> nanocrystals (NCs) into SiO<sub>2</sub> beads. The preparation procedure included the preparation of SiO<sub>2</sub>-coated Fe<sub>3</sub>O<sub>4</sub> NCs, the attachment of the CdTe NCs on the SiO<sub>2</sub>-coated Fe<sub>3</sub>O<sub>4</sub> NCs, the assembly of the CdTe NCs-attached Fe<sub>3</sub>O<sub>4</sub> NCs, and the growth of a SiO<sub>2</sub> shell. To prevent the photoluminescence (PL) quenching, Fe<sub>3</sub>O<sub>4</sub> NCs were coated with a thin SiO<sub>2</sub> layer before encapsulating into SiO<sub>2</sub> beads together with CdTe NCs. The CdTe NCs retained high PL efficiency (30 %) in dual functional SiO<sub>2</sub> beads. These SiO<sub>2</sub> beads also revealed superparamagnetic behavior. The result would be utilizable for further application because of their high PL efficiency and magnetic property. The strategy described here should give a useful enlightenment for the design and fabrication of multiple functional SiO<sub>2</sub> beads. Copyright © 2011 VBRI press.

**Keywords:** Bi-functional SiO<sub>2</sub> beads; iron oxide magnetic nanoparticle; semiconductor nanocrystals; sol-gel synthesis.



**Zhongsen Yang** got his B. Sc. at Jilin University, P. R. China in 1972. He has been working in the State Key Laboratory of Crystal Materials at Shandong University since 1972 as an engineer. His research focused on crystal materials, nanomaterials, magnetic and luminescent materials. Especially, his research is interesting in sol-gel chemistry, combustion synthesis, and photocatalysis.

## Introduction

Multifunctional nanomaterials have recently become an attractive research field. Functional composite nanomaterials with magnetism and fluorescence have been of great potential in biological applications such as magnetic resonance imaging (MRI) contrast agent, drug delivery carrier, cell sorting, and labeling [1–6]. The development of synthesis has enabled the production of magnetic, fluorescent microspheres consisted of various materials. A large number of methods have been developed to synthesize various magnetic and fluorescent microspheres involving emulsion, polymeric micelles, polymer-based particles, and silica-based particles [7]. Several reports have focused on the synthesis and investigation of dual functional nanomaterials such as hybrid and core-shell nanocomposites [8–12].

Superparamagnetic magnetite (Fe<sub>3</sub>O<sub>4</sub>) nanocrystals (NCs) are important for a diverse range of applications s

such as MRI, targeted drug delivery, and magnetic separation. Magnetic NCs offer great potential in biomedical applications. Because of unique optical properties, including narrow photoluminescence (PL) spectra, low photobleaching, and high resistance to chemical degradation, cadmium telluride (CdTe) NCs have attracted considerable attention over past decades. The multifunctional nanomaterials which were consisted of iron oxide and CdTe NCs can enable materials both the advantages of iron oxide nanoparticles and CdTe NCs. They showed great potential in biological applications [13]. However, an important factor for further development is homogeneity in particle sizes and contents of functional components, which will be required for advanced application and/or highly quantitative analysis [14]. The nanocomponents have to retain their initial properties after incorporation for applications.

Various approaches have been employed to prepare the multifunctional nanoparticles composed of iron oxide and luminescent NCs such as layer by layer [15] and sol-gel [16, 17] techniques. The direct attachment of magnetic and luminescent NCs during long and complicated synthesis procedures, however, drastically decreases the PL efficiency of the resulting NCs [18, 19]. Therefore, better preparing techniques are still needed to develop a novel preparation procedure for encapsulating these two kinds of NCs into SiO<sub>2</sub> beads without degrading the initially high PL efficiency. Since there are little papers published for SiO<sub>2</sub> beads with dual functions at the moment [17], SiO<sub>2</sub>

beads with dual functions have been an important research topic for medical and biological applications.

Because high PL efficiency is an important factor for supersensitive bioanalysis, we prepare dual functional  $\text{SiO}_2$  beads with CdTe and  $\text{Fe}_3\text{O}_4$  NCs by using a controlled sol-gel process here.  $\text{Fe}_3\text{O}_4$  NCs were first coated with a thin functional silica layer. CdTe NCs were then attached on the  $\text{SiO}_2$ -coated  $\text{Fe}_3\text{O}_4$  NCs (SFNCs) through mercapto groups as linkers. After that, the CdTe-attached  $\text{Fe}_3\text{O}_4$  NCs were assembled into nanocomposite particles. Finally, a  $\text{SiO}_2$  shell was deposited on the nanocomposite particles to create dual functional  $\text{SiO}_2$  beads. Herein, the synthesis and detailed structural, magnetic, and optical properties of these dual functional  $\text{SiO}_2$  beads were presented. These dual beads exhibited high PL efficiency and superparamagnetic behavior.

## Experimental

### Chemicals and materials

All chemicals were of analytical purity or of the highest purity available and used without purification. These chemicals were purchased from Sigma Aldrich except for ethanol, NaOH, and HCl. The pure water was obtained from a Milli-Q synthesis system.

### Synthesis of $\text{Fe}_3\text{O}_4$ NCs

Magnetite ( $\text{Fe}_3\text{O}_4$ ) NCs (MNCs) in an aqueous solution without any surfactants was prepared using a similar procedure in literature [20]. Briefly, 0.15 mL of HCl (12 M) was added in 10 mL of  $\text{H}_2\text{O}$  (by nitrogen gas bubbling for 30 min) with stirring. 0.519 g of  $\text{FeCl}_2$  and 0.13 g of  $\text{FeCl}_3$  were dissolved in the solution of HCl and  $\text{H}_2\text{O}$  with stirring. The resulting solution was added dropwise into 50 mL of 1.0 M NaOH solution under vigorous stirring. The precipitate was isolated by a magnet, and the supernatant was discarded by decantation.  $\text{H}_2\text{O}$  bubbled by  $\text{N}_2$  was added to the precipitate and the solution was decanted after centrifugation at 3500 rpm. The last procedure was repeated three times. 500 mL of 0.01M HCl solution was added to the precipitate (with stirring) to neutralize the anionic charges on the NCs. The sample was again separated by centrifugation (4500 rpm) and peptized by adding water.

### Preparation of CdTe NCs

Water-soluble thioglycolic acid (TGA)-capped CdTe NCs (TNCS) were prepared according to the procedure in literature [21, 22]. Briefly sodium borohydride was used to react with tellurium in water to prepare a sodium hydrogen telluride (NaHTe) solution by using a molar ratio of 3:1 for  $\text{NaHB}_4/\text{Te}$ . Fresh solutions of NaHTe were diluted by  $\text{N}_2$ -saturated deionized water for further use.

For the preparation of TNCS (red-emitting),  $\text{CdCl}_2 \cdot 2.5\text{H}_2\text{O}$  (0.4 mmol) and TGA (0.6 mmol) were dissolved in 25 mL of water to get a precursor solution followed by adjustment to a pH value of 10.8 by a NaOH solution of 1 M. The precursor solution was bubbled by  $\text{N}_2$  for 30 min. A fresh deoxygenated NaHTe solution was added in the above precursor solution with stirring. The

typical molar ratio of Cd:Te:TGA was 1:0.5:2. The mixture was subsequently refluxed for 5 h to fabricate TNCS.

### Magnetic and luminescent NCs encapsulated in $\text{SiO}_2$ beads

Dual functional  $\text{SiO}_2$  beads were prepared by using a three-step synthesis process. In step 1, a MNCs colloidal solution (0.5 mL) was added in ethanol (2 mL) with ammonia (6.25 wt%, 0.1 mL). Tetraethyl orthosilicate (TEOS, 2  $\mu\text{L}$ ) was then added in the solution with stirring for 2.5 h for getting SFNCs [23]. 3-mercaptopropyltrimethoxysilane (MPS, 0.2  $\mu\text{L}$ ) was then added with stirring for 10 h to obtain mercapto-functional surface. The ethanol was evaporated from the solution of functional SFNCs by  $\text{N}_2$  flowing. In step 2, TNCS were re-dispersed in  $\text{H}_2\text{O}$  with a pH of 10 which was adjusted by a NaOH solution. The re-dispersed TNCS were mixed with the SFNCs with stirring for 5 h. In step 3, TEOS of 10  $\mu\text{L}$  and ammonia (6.25 wt%, 0.05 mL) were added in the solution of CdTe-attached  $\text{Fe}_3\text{O}_4$  NCs with further reaction for 10 h. The resulting beads were separated by centrifuging at 19000 rpm for 10 min and washed by using ethanol for 3 times. Finally, the  $\text{SiO}_2$  beads were redispersed in  $\text{H}_2\text{O}$  for further characteristics. The stability of the resulting beads was investigated by adjusting the pH of solutions from 7 to 11.

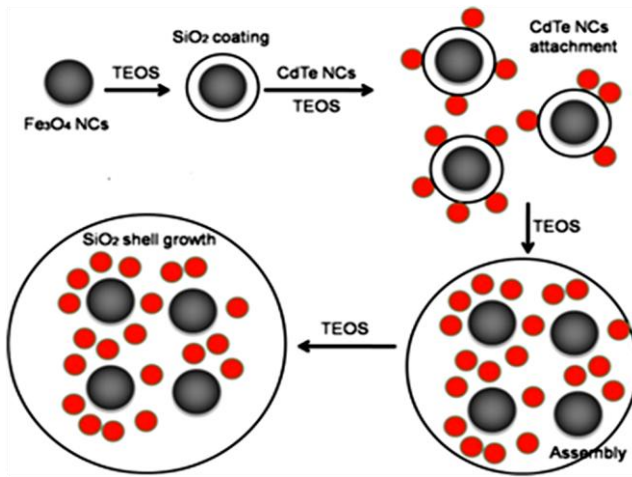
### Apparatus

Transmission electron microscopy (TEM) observations were carried out using JEM 2100 (JEOL Ltd.) and H-9000 (Hitachi) electron microscopes. The powder x-ray diffraction (XRD) pattern of samples was obtained with an x-ray diffractometer (D8-Avance, Bruker AXS). The absorption and PL spectra were taken using Hitachi U-4100 and F-4600 spectrometers. The PL efficiencies of NCs before and after incorporated in  $\text{SiO}_2$  beads were estimated with a method previously reported [24]. The PL efficiency of CdTe NCs at room temperature was estimated by comparison with Rhodamine 6G (PL efficiency of 95%) in an ethanol solution assuming its PL efficiency as 95%. The color image of sample was taken by using an Olympus IX 81 fluorescence microscope (Olympus Optical Co.).

## Results and discussion

Stöber synthesis of  $\text{SiO}_2$  particles with a diameter less than 1  $\mu\text{m}$  was first described in 1968 by an ethanol and ammonia solution [23]. In current experimental, a modified Stöber synthesis was used. **Scheme 1** illustrates the preparation procedure of dual functional  $\text{SiO}_2$  beads with  $\text{Fe}_3\text{O}_4$  and CdTe NCs. The preparation of the beads consists of three steps: the  $\text{Fe}_3\text{O}_4$  NCs coated with a thin functional  $\text{SiO}_2$  layer (step 1), the CdTe NCs attached to the functional  $\text{SiO}_2$ -coated  $\text{Fe}_3\text{O}_4$  NCs (step 2), the assembly of the CdTe-attached  $\text{Fe}_3\text{O}_4$  NCs into nanocomposite particles by the condensation of  $\text{SiO}_2$  monomers and the deposition of a  $\text{SiO}_2$  shell on the nanocomposite particles (step 3). During Step 1,  $\text{Fe}_3\text{O}_4$  NCs were coated with a thin  $\text{SiO}_2$  layer by a Stöber synthesis. In the one hand, the thin  $\text{SiO}_2$  layer prevented the CdTe NCs from PL quenching during incorporation. On the other, the thin  $\text{SiO}_2$  layer resulted in the size of resulting  $\text{SiO}_2$  beads decreased. To attach CdTe

NCs, the SFNCs were coated with a mercapto surface layer by using MPS. The mercapto groups in MPS resulted in the connection between CdTe NCs and SFNCs. For getting a high PL efficiency, the ethanol in the solution of the SFNCs was partly removed before step 2. During step 2, the mercapto groups on the SFNCs were easily linked with CdTe NCs since TGA molecules were removed from a CdTe colloidal solution. In step 3, the self-assembly of the CdTe-attached Fe<sub>3</sub>O<sub>4</sub> NCs occurred and SiO<sub>2</sub> shell coating was created further because of the hydrolysis and condensation of TEOS.



**Scheme 1.** Preparation procedure of SiO<sub>2</sub> beads with Fe<sub>3</sub>O<sub>4</sub> and CdTe NCs.

The formation mechanism of these dual functional SiO<sub>2</sub> beads was confirmed by TEM observation. **Fig. 1** shows the TEM images of Fe<sub>3</sub>O<sub>4</sub> NCs and SiO<sub>2</sub> beads with Fe<sub>3</sub>O<sub>4</sub> and CdTe NCs. The mean sizes of Fe<sub>3</sub>O<sub>4</sub> and CdTe NCs is 9 and 4 nm, respectively. The result is similar with that in literature [20]. The mean size of CdTe NCs is 3.9 nm according to the absorbance of CdTe NCs at first adsorption peak. On the edge of **Fig. 1** b2, several CdTe NCs were observed. However, it is difficult to recognize CdTe and Fe<sub>3</sub>O<sub>4</sub> NCs in the middle part of beads in Fig. b2 because of the overlap of well-developed lattices fringes. Two kinds of NCs were dispersed homogeneously in the center part of the beads. This means the self-assembly of the CdTe-attached Fe<sub>3</sub>O<sub>4</sub> NCs occurs before the growth of SiO<sub>2</sub> shell.

To further clarify that the CdTe NCs exist in these SiO<sub>2</sub> beads, we employed absorption and PL spectra for characterization. **Fig. 2** shows the absorption and PL spectra of SiO<sub>2</sub> beads with CdTe and Fe<sub>3</sub>O<sub>4</sub> NCs. The absorption and PL spectra of an initial CdTe colloidal solution are shown for comparison. The CdTe NCs exhibited a PL peak wavelength of 650 nm. The first absorption peak of the CdTe NCs in the beads did not show any change compared with that of the initial CdTe colloidal solution. However, the PL peak wavelength of the CdTe NCs in the beads revealed a red-shift and the full width at half-maximum (FWHM) from their PL spectra was reduced slightly compared with those of the initial CdTe colloidal solution. A similar phenomenon was observed from II-VI NCs-polymer rods [25]. This phenomenon is

ascribed that large CdTe NCs re-adsorbed the PL from small one. This means CdTe NCs were nearly arranged in a close packed manner on the surface of SiO<sub>2</sub>-coated Fe<sub>3</sub>O<sub>4</sub> NCs.

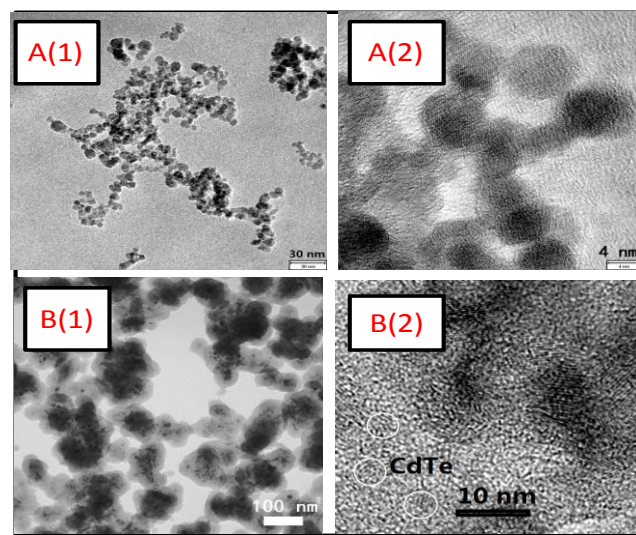


**Fig. 1.** TEM images: a (1) and a (2), Fe<sub>3</sub>O<sub>4</sub> NCs; b (1) and b (2), SiO<sub>2</sub> beads with Fe<sub>3</sub>O<sub>4</sub> and CdTe NCs. On the edge of b (2), several CdTe NCs were observed. However, it is difficult to recognize CdTe and Fe<sub>3</sub>O<sub>4</sub> NCs in the middle part of beads in b (2) because of the overlap of well-developed lattices fringes.

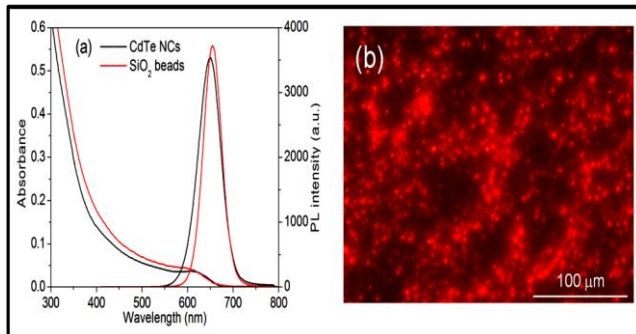


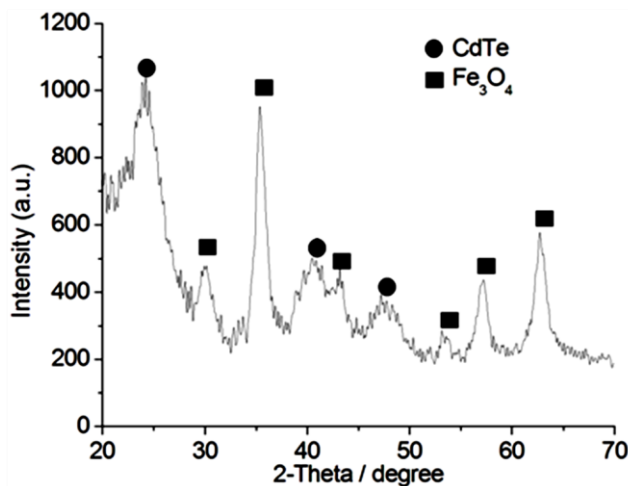
**Fig. 2.** (a) Absorbance and PL spectra of SiO<sub>2</sub> beads with Fe<sub>3</sub>O<sub>4</sub> and CdTe NCs. (b) Color image of dual functional SiO<sub>2</sub> beads with Fe<sub>3</sub>O<sub>4</sub> and CdTe NCs under 365 UV light. The absorbance and PL spectra of colloidal CdTe NCs are shown for comparison. The PL peak wavelength of CdTe NCs was 650 nm.

The PL efficiency of SiO<sub>2</sub> beads with CdTe and Fe<sub>3</sub>O<sub>4</sub> NCs was 30% while the initial PL efficiency of a CdTe colloidal solution was 45%. To the best of our knowledge, this PL efficiency is higher than that in literature. There have been a few reports on the PL efficiency of SiO<sub>2</sub> beads with magnetic and luminescent NCs. Ying's group prepared SiO<sub>2</sub> beads with connected Fe<sub>3</sub>O<sub>4</sub>-CdSe NCs (NCs with a very thin SiO<sub>2</sub> layer, several nanometers in total diameter), whose PL efficiency before and after SiO<sub>2</sub> coating was 13–18% and 8–10%, respectively [26]. These values are higher than the PL efficiency of 3.2% reported for FePt–CdS NCs [27]. Under UV light, these beads showed bright emission (Fig. 2b), making them well suited for biological and medical applications. In these cases, the connection of two kinds of NCs resulted in the decrease of PL efficiency. In addition, iridium-complex-functionalized

$\text{Fe}_3\text{O}_4/\text{SiO}_2$  core-shell beads (~50 nm) retaining a PL efficiency of 10% was reported [28]. Guo *et al.* reported  $\text{SiO}_2$ -coated  $\text{Fe}_3\text{O}_4/\text{SiO}_2/\text{CdTe}$  beads (~160 nm) [29]. In that case, the efficiency of the initial colloidal TNCs was estimated to be 30-40%. They did not, however, indicate the PL efficiency of these beads. In contrast, we prepared dual functional  $\text{SiO}_2$  beads with multiple  $\text{Fe}_3\text{O}_4$  and CdTe NCs. The approach offers tremendous potential for maintaining the initial PL properties of NCs.

Two reasons resulted in that the CdTe NCs retained PL efficiency in dual functional  $\text{SiO}_2$  beads. One was the thin  $\text{SiO}_2$  layer on the  $\text{Fe}_3\text{O}_4$  NCs obtained by step 1. This caused the  $\text{Fe}_3\text{O}_4$  NCs to separate with CdTe NCs after incorporating in the beads. The thin  $\text{SiO}_2$  layer then protected the CdTe NCs against PL quenching. The other reason was the partly movement of ethanol from the solution of  $\text{SiO}_2$ -coated  $\text{Fe}_3\text{O}_4$  NCs after step 1.

To confirm the existence of  $\text{Fe}_3\text{O}_4$  NCs in the dual functional  $\text{SiO}_2$  beads, Fig. 3 shows the powder XRD pattern of as-prepared dual functional  $\text{SiO}_2$  beads. The position of six diffraction peaks match well with a cubic spinel structure of magnetite. Three other diffraction peaks are indexed to a cubic CdTe.



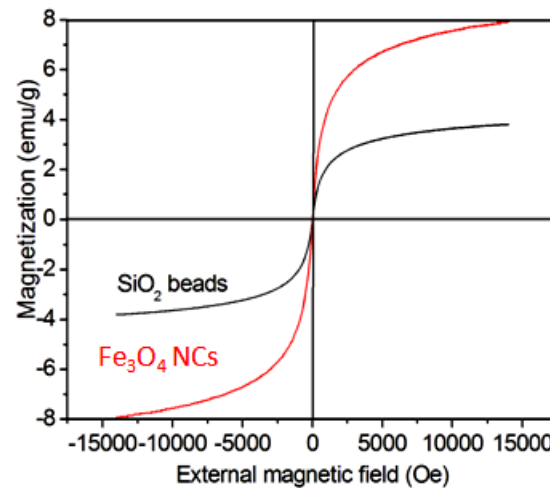
**Fig. 3.** XRD pattern of dual functional  $\text{SiO}_2$  beads. All of the diffraction peaks were indexed to a cubic  $\text{Fe}_3\text{O}_4$  or CdTe.

Fig. 4 shows the field-dependent magnetization plots of  $\text{Fe}_3\text{O}_4$  NCs and  $\text{SiO}_2$  beads with CdTe and  $\text{Fe}_3\text{O}_4$  NCs. This field-dependent magnetization plot indicates the beads revealed a super-paramagnetic behavior at room temperature. The magnetic saturation values of  $\text{Fe}_3\text{O}_4$  NCs and the beads are 7.9 and 3.8 emu/g, respectively. In addition, stability investigation demonstrated the dual functional  $\text{SiO}_2$  beads retained their initial PL efficiency in the pH range of 7 to 10.5. As a result, these dual functional  $\text{SiO}_2$  beads should be utilizable for further applications.

## Conclusion

Water-soluble  $\text{SiO}_2$  beads with CdTe and  $\text{Fe}_3\text{O}_4$  NCs were synthesized through a three-step sol-gel synthesis. A functional  $\text{SiO}_2$  layer with mercapto groups was as a linker between two kinds of NCs. Such  $\text{SiO}_2$  layer resulted in dual functional  $\text{SiO}_2$  beads with a high PL efficiency of 30%.

Because these brightly luminescent beads exhibited high stability and super-paramagnetic behavior, we will next focus on their bio-applications, such as magnetic resonance imaging, drug delivery, cell labeling, and magnetic cell separation.



**Fig. 4.** Field-dependent magnetization plots of  $\text{Fe}_3\text{O}_4$  NCs  $\text{SiO}_2$  beads contained CdTe and  $\text{Fe}_3\text{O}_4$  NCs. The magnetic saturation values of  $\text{Fe}_3\text{O}_4$  NCs and the beads are 7.9 and 3.8 emu/g, respectively.

## Acknowledgements

This work was supported in part by projects from National Science Foundation of China (50972081) and Natural Science Foundation of Shandong Province (Y2008F32).

## Reference

- Huh, Y. M.; Jun, Y. M.; Song, H. T.; Kim, S.; Choi, J. S.; Lee, J. H.; Yoon, S.; Kim, K. S.; Shin, J. S.; Suh, J. S.; Cheon, J. *J. Am. Chem. Soc.* **2005**, *127*, 12387.  
DOI: [10.1021/ja052337c](https://doi.org/10.1021/ja052337c)
- Giri, S.; Trewyn, B. G.; Stellmarker, M. P.; Lin, V. S. Y. *Angew. Chem. Int. Ed.* **2005**, *44*, 5038.  
DOI: [10.1002/anie.200501819](https://doi.org/10.1002/anie.200501819)
- Kim, J.; Lee, J. E.; Lee, J.; Jang, Y.; Kim, S. M.; An, K.; Yu, J. H.; Hyeon, T. *Angew. Chem., Int. Ed.* **2006**, *45*, 4789.  
DOI: [10.1002/anie.200504107](https://doi.org/10.1002/anie.200504107)
- Sen, T.; Sebastianelli, A.; Bruce, I. J. *J. Am. Chem. Soc.* **2006**, *128*, 7130.  
DOI: [10.1021/ja061393q](https://doi.org/10.1021/ja061393q)
- Singhal, R. P.; Choi, J. W. *Adv. Mat. Lett.* **2010**, *1*, 83.  
DOI: [10.5185/amlett.2010.4109](https://doi.org/10.5185/amlett.2010.4109)
- Shukla, S. K.; Bharadvaja, A.; Tiwari, A.; Parashar, G. K.; Dubey, G. C. *Adv. Mat. Lett.* **2010**, *1*, 129.  
DOI: [10.5185/amlett.2010.3105](https://doi.org/10.5185/amlett.2010.3105)
- Salgueirinó-Maceira, V.; Correa-Duarte, M. A. *Adv. Mater.* **2007**, *19*, 4131.  
DOI: [10.1002/adma.200700418](https://doi.org/10.1002/adma.200700418)
- Yu, H.; Chen, M.; Rice, P. M.; Wang, S. X.; White, R. L.; Sun, S. *Nano Lett.* **2005**, *5*, 379.  
DOI: [10.1021/nl047955q](https://doi.org/10.1021/nl047955q)
- Shi, W.; Zeng, H.; Sahoo, Y.; Ohulchansky, T. Y.; Ding, Y.; Wang, Z. L.; Swihart, M.; Prasad, P. N. *Nano Lett.* **2006**, *6*, 875.  
DOI: [10.1021/nl0600833](https://doi.org/10.1021/nl0600833)
- Salgueirinó-Maceira, V.; Correa-Duarte, M. A.; Spasova, M.; Liz-Marzañ, L. M.; Farle, M. *Adv. Funct. Mater.* **2006**, *16*, 509.  
DOI: [10.1002/adfm.200500565](https://doi.org/10.1002/adfm.200500565)
- Yi, D. K.; Selvan, S. T.; Lee, S. S.; Papaefthymiou, G. C.; Kundaliya, D.; Ying, J. Y. *J. Am. Chem. Soc.* **2005**, *127*, 4990.  
DOI: [10.1021/ja0428863](https://doi.org/10.1021/ja0428863)
- Singha, V.; Singha, S. K.; Pandeya, S.; Sanghi, R. *Adv. Mat. Lett.* **2010**, *1*, 40.  
DOI: [10.5185/amlett.2010.4107](https://doi.org/10.5185/amlett.2010.4107)

13. Li, X. Z.; Wang, L.; Zhou, C.; Guan, T. T.; Li, J.; Zhang, Y. H. *Clin. Chim. Acta*, **2007**, *168*, 378.  
DOI: [10.1016/j.cca.2006.11.013](https://doi.org/10.1016/j.cca.2006.11.013)
14. Nagao, D.; Yokoyama, M.; Yamauchi, N.; Matsumoto, H.; Kobayashi, Y.; Konno, M. *Langmuir*, **2008**, *24*, 9804.  
DOI: [10.1021/la801364w](https://doi.org/10.1021/la801364w)
15. Hong, X.; Li, J.; Wang, M. J.; Xu, J. J.; Guo, G.; Li, J. H.; Bai, Y. Li; T. J. *Chem. Mater.* **2004**, *16*, 4022.  
DOI: [10.1021/cm049422o](https://doi.org/10.1021/cm049422o)
16. Xiao, Q.; Xiao, C.; *Nanoscale Res. Lett.* **2009**, *4*, 1078.  
DOI: [10.1007/s11671-009-9356-0](https://doi.org/10.1007/s11671-009-9356-0)
17. Wang, W.; Wang, C.; Dou, W.; Ma, Q.; Yuan, P.; Su, X. *J. Fluoresc.* **2009**, *19*, 939. DOI: [10.1007/s10895-009-0493-8](https://doi.org/10.1007/s10895-009-0493-8)
18. Wang, D.; He, J.; Rosenzweig, N.; Rosenzweig, Z. *Nano Lett.* **2004**, *4*, 409. DOI: [10.1021/nl035010n](https://doi.org/10.1021/nl035010n)
19. Roullier, V.; Grasset, F.; Boulmedais, F.; Artzner, F.; Cador, O.; Marchi-Artzner, V. *Chem. Mater.* **2008**, *20*, 6657. DOI: [10.1021/cm801423r](https://doi.org/10.1021/cm801423r)
20. Kang, Y. S.; Risbud, S.; Rabolt, J. F.; Stroeve, P. *Chem. Mater.* **1996**, *10*, 2209. DOI: [10.1021/cm960157j](https://doi.org/10.1021/cm960157j)
21. Wolcott, A.; Gerion, D.; Visconate, M. Sun, J.; Schwartzberg, A.; Chen, S.; Zhang, Z. *J. Phys. Chem. B*, **2006**, *110*, 5779. DOI: [10.1021/jp057435z](https://doi.org/10.1021/jp057435z)
22. Tomasulo, M.; Yildiz, I.; Raymo, F. M. *J. Phys. Chem. B*, **2006**, *110*, 3853. DOI: [10.1021/jp060185h](https://doi.org/10.1021/jp060185h)
23. Stöber, W.; Fink, A.; Bohn, E. J. *Colloid Interface Sci.* **1968**, *26*, 62.
24. Crosby, G. A.; Demas, J. N. *J. Phys. Chem.* **1971**, *75*, 991. DOI: [10.1021/j100678a001](https://doi.org/10.1021/j100678a001)
25. Lee, J.; Sundar, V. C.; Heine, J. R.; Bawendi, M. G.; Jensen, K. F. *Adv. Mater.* **2000**, *12*, 1102. DOI: [10.1002/1521-4095\(200008\)12:11<1102::AID-ADMA1102>3.0.CO;2-1](https://doi.org/10.1002/1521-4095(200008)12:11<1102::AID-ADMA1102>3.0.CO;2-1)
26. Selvan, S. T.; Patra, P. K.; Ang, C. Y.; Ying, J. Y. *Angew. Chem. Int. Ed.* **2007**, *46*, 1448. DOI: [10.1002/anie.200604245](https://doi.org/10.1002/anie.200604245)
27. Gu, H.; Zheng, R.; Zhang, X. X.; Xu, B. *J. Am. Chem. Soc.* **2004**, *126*, 5664. DOI: [10.1021/ja0496423](https://doi.org/10.1021/ja0496423)
28. Lai, C. W.; Wang, Y.; Lai, C. H.; Yang, M.; Chen, C.; Chou, P.; Chan, C.; Chi, Y.; Chen, Y.; Hsiao, J. *Small*, **2008**, *4*, 218. DOI: [10.1002/smll.200700283](https://doi.org/10.1002/smll.200700283) Key: citeulike:2793283
29. Guo, J.; Yang, W.; Wang, C.; He, J.; Chen, J. *Chem. Mater.* **2006**, *18*, 5554. DOI: [10.1021/cm060976w](https://doi.org/10.1021/cm060976w)

## ADVANCED MATERIALS Letters

Publish your article in this journal

**ADVANCED MATERIALS Letters** is an international journal published quarterly. The journal is intended to provide top-quality peer-reviewed research papers in the fascinating field of materials science particularly in the area of structure, synthesis and processing, characterization, advanced-state properties, and applications of materials. All articles are indexed on various databases including [DOAJ](#) and are available for download for free. The manuscript management system is completely electronic and has fast and fair peer-review process. The journal includes review articles, research articles, notes, letter to editor and short communications.

